

Analysis of Some Solutions that Improve Performances of Plate-Type Electrostatic Precipitators

GABRIEL NICOLAE POPA¹ IOAN ȘORA² VICTOR VAIDA³ IOSIF POPA¹ SORIN DEACONU¹

¹Department of Electrical Engineering and Industrial Informatics

²Department of Electrical Engineering

Politechnica University Timișoara

Str. Revoluției, no.5, Hunedoara

³ Thermal Power Plant, Mintia-Deva

ROMANIA

gabriel.popa@fih.upt.ro http://fih.upt.ro/np/depelectro/dep_electro.html

Abstract: - The plate-type electrostatic precipitators are used in burning industry applications and can treat large gas flows. The paper presents the maximum ionization distance, analytic and graphic, near discharge wires depending on the voltage supply frequency and the discharge wires radius. A problem of this type of precipitator is difficulty to collect high resistivity fly ash. In the inlet section the fly ash resistivity is moderate and it is necessary to charge dust particles as many as possible. It is useful to use traditional dc energization. For the middle section and especially for outlet section, where the fly ash resistivity is high, it is necessary another supply solution for section because the charging particle decrease when is used traditional dc energization. The paper presents analysis of different types supplies of ESP sections. The intermittent energization of sections can be a cheap solution to middle and outlet section (without change the power supply structure, it is necessary the change of the automatic voltage control unit). It is important to know the current-voltage characteristics to obtain the optimal control of the amplitude, the voltage shape, the input power and the collection efficiency. With comparative analyze of the measured and computed characteristics, with different mathematical model of current-voltage characteristics, it can be found which models estimate the current-voltage characteristics for plate-type electrostatic precipitators.

Key-Words: plate-type electrostatic precipitators, dc energization, intermittent energization, current-voltage characteristics, mathematical models

1 Introduction

In the most burning applications it is used the plate-type electrostatic precipitators (ESP) because have following advantages: can be sized for large gas flow, can operate in a wide range of temperatures and the collection efficiency is high.

In ESP, the gas particles from the burning process, are passed through electric field where it is generating electrical charges (through Corona effect) attaching to gas particles. The discharge wires are connected to negative (-) polarity of power supply, and electric charge of gas particles is negative. Thus, the gas particles are deflected by the electric field from the discharge wires to collecting plates that are connected to earth. The gas particles are removed to collecting plates into receiving hoppers by mechanical shocks. The ESPs are made from a number by 3÷4 of series sections, each of them is energized by its own transformer rectifier set and has its own hoppers [1,2].

Corona is the ionization of gas molecules by high energy electrons in the region of a strong electric field [2,3,4].

The electrical current is formed by gas ions from space between electrodes. The velocity of the gas ions is proportional with electrical field applied and the constant called electrical mobility of gas ions [1].

The onset corona discharge occurs over a wide range of voltage. For traditional dc energized ESP sections (most use method), the corona currents are relatively small (mA) for high applied voltage (tens of kV). The current increase nearly proportional with applied voltage until breakdown occurs [4,5].

The electric field strength between the electrodes (the discharge wires and the collecting plates) depends on two factors: the surface charges on the electrodes (due the applied voltage) and the space charge component (due the ions from electrode spacing) [1,6].

A number of numerical methods have been proposed to solve problems for complex discharge wire electrode geometries using finite difference,

finite elements or charge simulations software [6,7,8]. It has been developed finite difference method to compute the steady state corona current distribution in the ESP sections to compute maximum corona current which can be carried in different geometric configuration of electrodes section [7].

Traditional dc energization of ESP sections are characterised by low current corona and the ionization processes is very small near the discharge wires [1,5,9].

The efficiency of ESP may be improves by electrical or mechanical means. Because a mechanical upgrade of ESP sections is too expensive, a solution to improve collection efficiency is to modify electrical equipment and/or control unit. The most ESPs are supply by single phase thyristors high voltage power supplies that represent considerably lower investments cost for ESP supplies [10,11].

The collection of dust particles in ESP sections is determined by migration velocity w (particle velocity perpendicular to the collecting plates). The supply voltage and the discharge wires geometry have an important effect on the migration velocity. Irregular discharge wires (e.g. barbed plate, barbed wire and spike band) are useful to corona electrodes [12].

The main goal of the control unit is to maintain the voltage from ESP sections near Corona voltage. For this reason the voltage must be rise until occur discharges in ESPs. After a discharge, is come the period of recover voltage that must be shorter after the discharge. To create an optimal control algorithm, it is important to know the current-voltage characteristics for ESPs [1,6,13].

The energization of ESP section is limited by the following conditions [1,14,15]:

- sparking that limit the peak voltage and is affected by other parameters. The electrical energy increase and the dust collection reduced and the power must be turned off to quench this arc;
- back corona when the dust emission increase due the production of opposite polarity ions and the energy consumption increase;
- equipment capacity that depends on peak voltage and average voltage;
- SO₃ conditioning through injection SO₃ into the gas (before ESP) will reduce the dust resistivity and prevent back corona;
- moisten of dust will act to reduce the dust resistivity and minimize back corona.

2 Ionization distance from discharge wires

An important problem is the determination of spatial charge distance. Let be consider a ion which has the mobility k_i and it is place in alternating field with frequency f , by electric field strength E , the field is made by a discharge wires with radius r_e , that is connected at high potential that determine Corona discharge [1,2]:

$$v = k_i \cdot E \quad (1)$$

The ion speed may be also compute depending on the distance by discharge wire r and the time t :

$$v = \frac{dr}{dt} \quad (2)$$

The electric field strength E it is not constant and depends by discharge wire radius r_e , the distance r until place where is calculate the electric field strength E and by the electric field strength at the discharge wire surface E_e :

$$E = E_e \frac{r_e}{r} \quad (3)$$

From (1), (2) and (3) results:

$$k_i \cdot E_e \frac{r_e}{r} = \frac{dr}{dt} \quad (4)$$

After integration (4) became:

$$t_{10}^2 = \frac{1}{k_i \cdot E_e \cdot r_e} \cdot \frac{r^2}{2} \Big|_{r_e}^{r_{max}} \quad (5)$$

$$f = \frac{1}{T} \quad (6)$$

From (5) and (6) can be compute r_{max} :

$$r_{max} = \sqrt{r_e^2 + \frac{k_i \cdot E_e \cdot r_e}{f}} \quad (7)$$

To compute the maximum ionization distance r_{max} let be consider the following example – from industry [1,5]: $k_i=2$ [cm²/(V·s)], $E_e = 40$ [kV/cm], $r_e \in (0.01-0.2)$ [cm], and $f \in (0.05-50)$ [kHz]. With these data and with MatLab 5.3 software, are made two graphics: r_{max} depends on discharge wire radius r_e and electric field frequency f , on frequency domains. In fig.1.a is the frequency domain 50-500 [Hz] and in fig.1.b is the frequency domain 0.5-50 [kHz]. To produce large numbers of charge carriers on surface of discharge wires a critical field strength has to be overcome when feed with negative supply. Because of natural radioactivity some molecules become ionized and recombine immediately. The electrons will be accelerated and determine new ionizations through collision of gas molecules. If electrons did not attach by gas molecules, then electrons determine exciting molecules that encourage an easy ionization at a future collisions. At a bigger

distance by discharge wire, the electrons have not a high speed and these will be attach by dust particles that are lay down on collecting plate (that are connected to earth). The positive ions that appear in the collision time move to discharge wire and determine new electron emissions.

If the discharge wire is positive, the electrons from space between electrodes will be accelerated, and will be collision with gas molecules and occur positive ions that are move through collecting plate that are connected to earth.

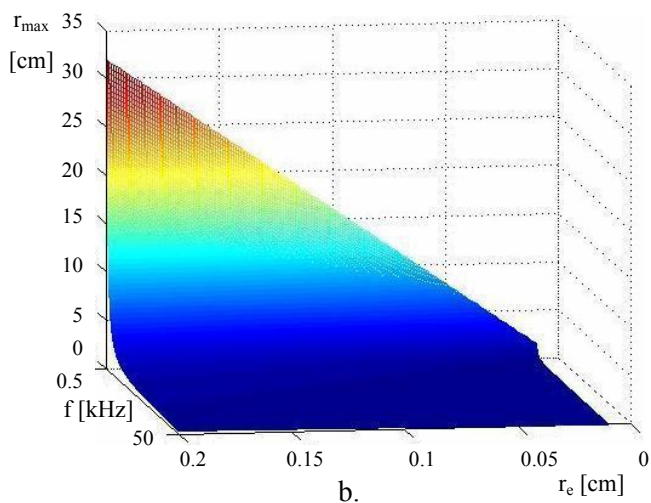
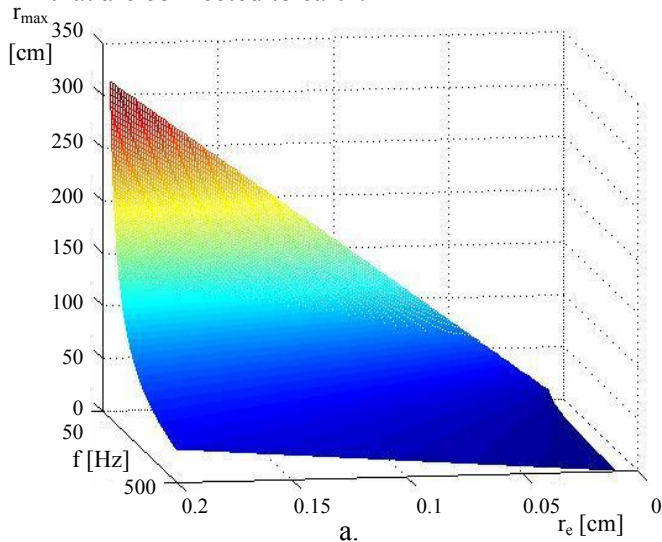


Fig.1. Maximum distance ionization depending on frequency and discharge wire radius

The gap between electrodes (discharge wires and collecting plates) depends on voltage frequency when the ESP section is supply with alternating voltage. If the distance between electrodes is small enough and the ions arrive to opposite polarity electrode into half period, then the Corona discharge is the same with negative or positive supply of discharge wires. If the distance between electrodes is bigger, the spatial charge carriers keep

the polarity with the voltage decrease. The ions guide to electrodes until the discharge wire potential change the polarity. Thus, appear an oscillation trajectory of ions [1,6,9].

3 DC and intermitent energization of ESP sections

The signals used by the control unit are presented in fig.2.

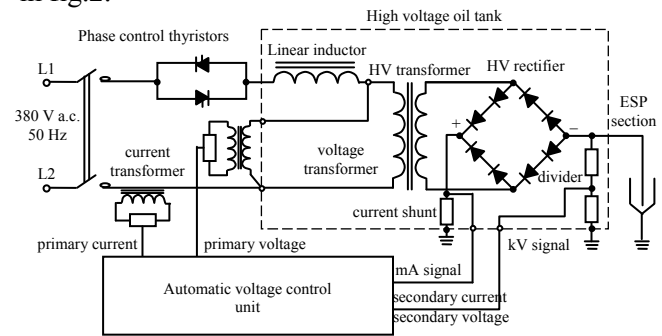


Fig.2. Power supply of ESP section

The traditional dc energization is obtained with power supply presented in fig.2. To obtain dc energization can be also used high voltage boost conevertors [10,16]. The line voltage is controlled by a thyristor controller, and then it is applied to the primary of high voltage transformer. The high voltage it is rectified by high voltage rectifier bridge, and the rectified secondary voltage is applied to the discharge wires from precipitator section. The rectified secondary voltage is connected (- to discharge wires and collecting plates are earthed) to generate negative corona in the precipitator section. An inductor is connected in series with thyristors to increase the short-circuit impedance during the events from ESP sections (sparking, arcing, or short-circuit). The high voltage can be also measured with another type of divider [17]. The firing angle of the thyristors must be controlled automatically because most of processes in ESP sections are subject to both slow and fast changes in the operating conditions. Some parameters like gas temperature and humidity, ash resistivity and fuel characteristics are change frequently [18,19].

The control units are based on microprocessors (or microcontrollers) and peripheral circuits which offer powerful performance.

The control corona currents from precipitator sections are made through using primary and secondary values (voltages and currents). Sometimes, the installation of opacitymeter in the stack is used to monitoring the dust emission and has two functions [1,10]:

- to optimizing the operation of ESP sections;
- to save the energy under easy conditions.

The rms and the mean current through ESP section are:

$$I_{0rms} = \sqrt{\frac{1}{T} \int_0^T i_0^2(t) dt} , \quad (8)$$

$$I_{0mean} = \frac{1}{T} \int_0^T |i_0(t)| dt . \quad (9)$$

Another important quantity are, the peak factor k_p and the form factor k_F of the precipitator section:

$$k_p = \frac{I_{0peak}}{I_{0mean}} , \quad (10)$$

$$k_F = \frac{I_{0rms}}{I_{0mean}} . \quad (11)$$

Identically, can be determine these quantities for precipitator section voltage.

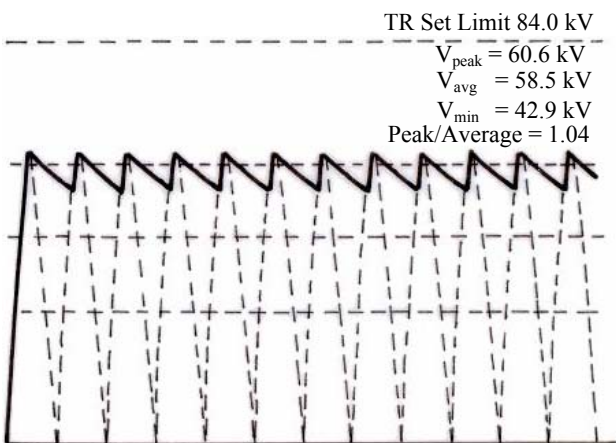


Fig.3. Voltage shape in ESP section for traditional dc energization

Intermittent energization is a method to saving energy and improving the collection efficiency for high resistivity dust. It is used the same electrical equipment employed in traditional dc energization. The control unit suppress a number of even half-cycle of primary current.

The degree of intermittence (D) is defined as a number of current pulses in one energization duty cycle divided by the number of half cycles included the energization cycle.

The current for intermittent energization (I_{IE}) depending on current for traditional dc energization (I_{DC}), a parameter k ($1 \div 1.5$), and degree of intermittence D [1]:

$$I_{IE} = k \cdot \frac{I_{DC}}{D} . \quad (12)$$

$D > 3$ (odd, up to 25), that demonstrate low current for intermittent energization and power consumption of ESP is reduced.

Through dust resistivity measure, the energization controller automatically detects the high resistivity ash and provides the optimum ESP performance under different dust resistivity conditions [15].

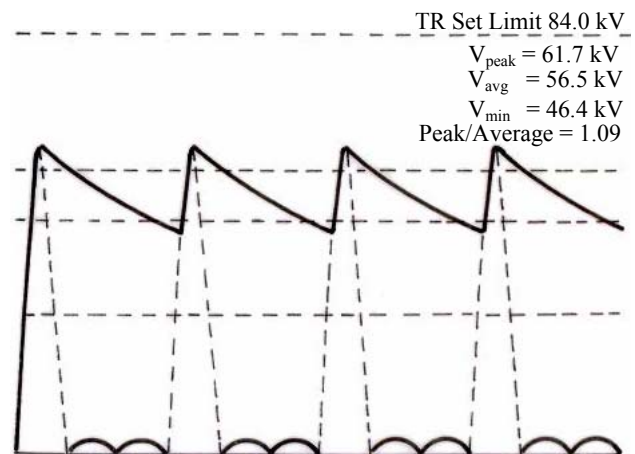


Fig.4. Voltage shape in ESP section for intermittent energization (D=1:3)

If it is noted with q_i [g/m^3] the inlet electrostatic precipitators dust concentration and with q_o [g/m^3] the outlet electrostatic precipitators dust concentration, the ESP collection efficiency η [-] is:

$$\eta = \frac{q_i - q_o}{q_i} = 1 - \frac{q_o}{q_i} , \quad (13)$$

$$\alpha = \frac{S_c}{Q} , \quad (14)$$

α [$m^2/m^3/s$] is specific collecting area, S_c [m^2] is electrostatic precipitator collecting plates area, and Q [m^3/s] is the gas volume flow. The Deutsch equation for electrostatic precipitator collection efficiency is [1,2,20]:

$$\eta = 1 - e^{-w \cdot \alpha} , \quad (15)$$

w [m/s] is migration velocity of dust particles towards collecting plates.

4 Analysis of different types supplies for ESP sections

The power consumption of industrial ESP are be in the range of hundred of kW [19].

At the inlet section (first section), the distribution of particles is very inhomogeneous and the concentration is very high. The dust resistivity is low to moderate ($< 10^{10}$ [$\Omega \cdot cm$]) and is necessary to charge particles as many is possible through high corona currents. The back corona rarely occurs in the inlet section.

In the middle section the distribution of particles becomes homogeneous and the concentration of dust

particles is lower. The dust resistivity increase and the back corona occurs more frequent and it is necessary other time of energization (intermitent or pulse energization). The average diameter of dust particles is less than in the first section.

In the outlet section (last section) the concentration of dust particles is low, but the dust particles is smaller and the dust resistivity is high ($>10^{11}$ [$\Omega\cdot\text{cm}$]). Back corona often happens in the outlet section. For high resistivity is necessary intermitent or pulse energization.

The ESPVI 4.0.a software is an ESP performance prediction model, is sponsored by the United States Environmental Agency. This software has a lot of parameters of ESP [21]:

- a. the general electrostatic precipitator parameters;
- b. the electrical parameters for every section;
- c. the gas parameters;
- d. the dust parameters.

It is mentioned that this software automatic executes adapting of parameters for respect of the connection among parameters. For each parameter are physic limitations.

Table 1

The general parameters of the dust and the gas

Resistivity [$\Omega\cdot\text{cm}$]	Gas flow [m^3/s]	Velocity of gas [m/s]	Temperature [$^{\circ}\text{C}$]
$2\cdot 10^{10}$	114.4	0.592	145
Pressure [atm]	The inlet dust concentration [mg/m^3]	Dynamic viscosity [$\text{kg}/(\text{m}\cdot\text{s})$]	
1	24.61	$2.6\cdot 10^{-5}$	

Table 2

The electrical parameters of the plate-type electrostatic precipitators

Section	Voltage [kV]	Current density [nA/cm^2]	Peak voltages [kV]
1	47	16	92
2	43	11	92
3	39	12.9	92
4	44	36.9	92
Section	Peak currents [A]	Type of energization	
1	1.8	traditional dc energization	
2	1.8	traditional dc energization	
3	1.8	traditional dc energization	
4	1.8	traditional dc energization	

The simulations are made for ESPs from a thermal power plant, that have the maximum gas flow $Q=650000$ [m^3/h], the apparent power $S=166$ [kVA]. The ESPs have four identical sections. The main constructive data for one section are: plate area $S_{\text{platearea}}=4868.5$ [m^2]; the distance between the collecting plates and the discharge wires $s = 0.175$ [m]; length $L = 4.32$ [m]; height $h = 12$ [m]; width $l = 16.1$ [m] [2,22,23].

The discharge wires are disposing in ducts and are equidistances. First discharge wire is place at 9 [cm] from the duct inlet, and the distance among the discharge wires is by 14 [cm].

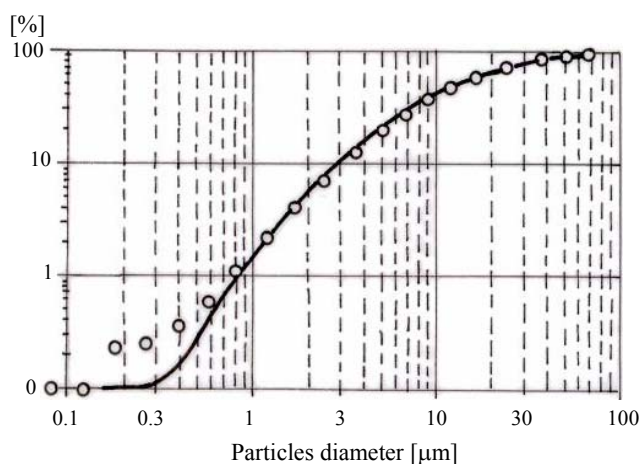
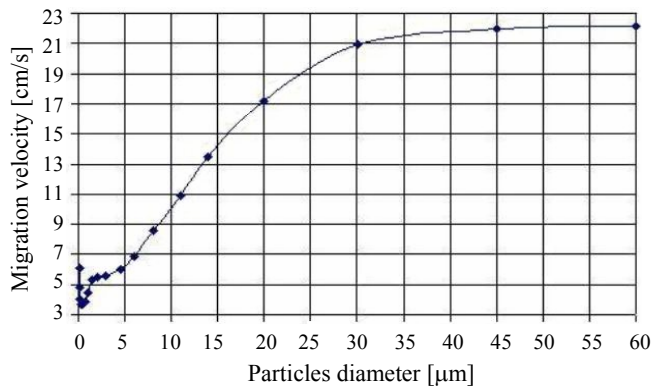


Fig.5. Gas particles masses distributions depending on gas particles average diameter

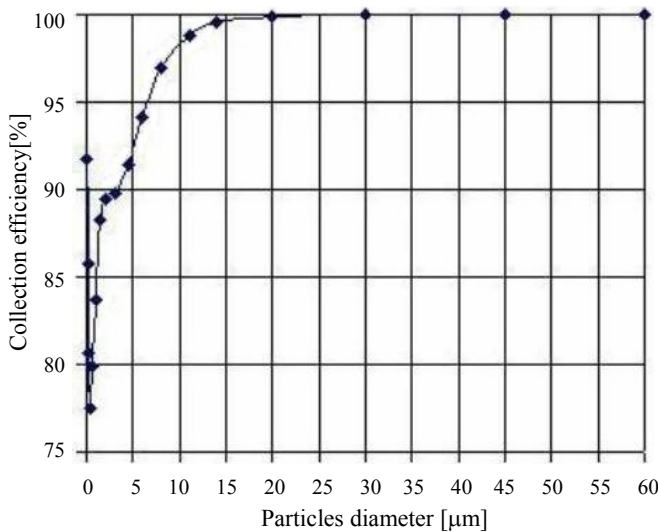
From fig.5 it is observe that in volume unity of residual gas, the gas particles with diameter between 1[μm] and 60 [μm] have bigger masses. Although the gas particles masses with diameter under 1[μm] have less value that the other particles masses, its number is bigger. The ESP collect more difficult the particles with diameter under 10 [μm] [18].

The collection efficiencies of ESP from a thermal power plant were measured [22] and simulated for ten technological situations, for two ESP noted with ESP1A and ESP1B, are different each other through inlet dust concentrations, that are noted in table 4 from I to V. The relative errors of collection efficiency are very small that demonstrate the performance of the ESPVI 4.0.a software on conditions that are using the real technological (from industry) and electrical parameters.

The migration velocity and collection efficiency are small for dust particles with mean diameters under 5[μm], and are big for dust particles with mean diameters over 10[μm]. Thus, at traditional energization, the collecting of dust particles with diameter very small (under 5[μm]) is lower.



a.



b.

Fig.6. Migration velocity (a) and collection efficiency (b) depending on particles average diameter for traditional dc energization for all ESP section

It was simulated the collection efficiency (fig.6) for ESP depending on discharge wires, when the

other geometrical dimensions are the same (it was modify only the number of discharge wires from sections).

Table 3

The types of energizations used in measurements and simulations of electrostatic precipitators sections

Section	Case a	Case b
1	traditional dc energization	traditional dc energization
2	traditional dc energization	traditional dc energization
3	traditional dc energization	intermitent 1:03
4	traditional dc energization	intermitent 1:03

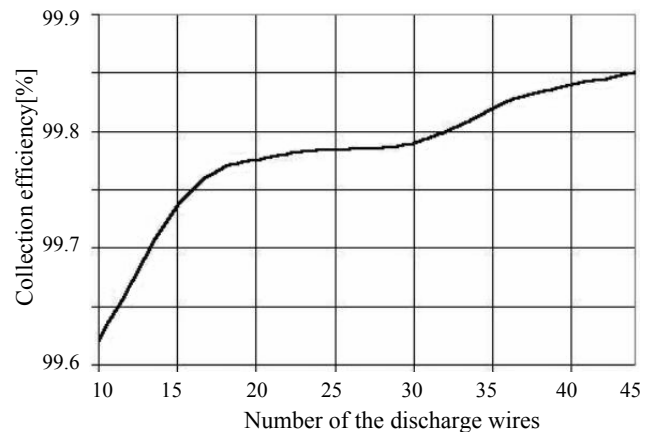


Fig.7. Collection efficiency depending on discharge wires in the duct

It was simulated the collection efficiency (fig.7) for ESP depending on distance between the collecting plates and the discharge wires, when the other geometrical dimensions are the same (it was modify only the distance between the discharge wires and collecting plates).

Table 4

The collection efficiency for the types of energizations presented in table 3

Cases	Inlet dust concentration q_i [g/m ³]	Outlet dust concentration q_o [g/m ³]	Collection efficiency			Relative error $\frac{ \eta_s - \eta_m }{\eta_m} \cdot 100$ [%]
			Measured η_m [%] (6)	Simulated η_s [%]		
				Case a (table 3)	Case b (table 3)	
ESP 1A case I	24.27	0.059	99.76	99.78	-	0.02
ESP 1B case II	22.235	0.06	99.73	99.78	-	0.05
ESP 1A case III	24.61	0.056	99.77	99.79	-	0.02
ESP 1B case IV	20.84	0.053	99.75	99.79	-	0.04
ESP 1A case V	26.915	0.083	99.69	99.8	-	0.11
ESP 1B case VI	28.795	0.085	99.7	99.78	-	0.08
ESP 1A case VII	26.915	0.08	99.7	-	99.83	0.13
ESP 1B case VIII	28.795	0.092	99.68	-	99.83	0.15
ESP 1A case IX	26.915	0.061	99.77	-	99.83	0.06
ESP 1B case X	28.795	0.087	99.7	-	99.83	0.13

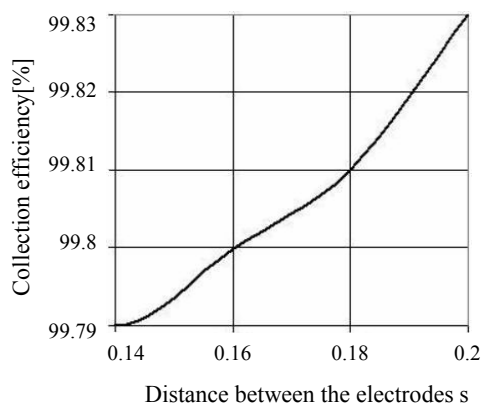


Fig.8. Collection efficiency depending on distance between electrodes (discharge wires and collecting plates)

Increasing the distance between electrodes resulted in decreased collection area. Through increasing sectionalization, the inlet section is used for low resistivity fly ash and the middle and the outlet section are used for high resistivity fly ash.

It is possible to addition a precharge field provides significant improvements in collection (especially for submicron dust particles) [18].

Wide plate spacing between electrodes, without an increase in overall ESP size and voltage supplies, will not increase the collection efficiency.

When high resistivity fly ash is processed a wide plate spacing is necessary (usually, 0.2 [m]). The back corona is limited by increasing electrode spacing [20].

Then, it was simulated the collection efficiency (fig.8) for ESP depending on types of sections energizations for ESP with four sections. In fig.8 was noted with DC – energize of sections with continuous voltage (ideal); 1:01 energize with traditional dc energization; 1:02 energize with monowave rectifying voltage (with only one diode); 1:03 intermitent energization with order 3 (D=3), so on.

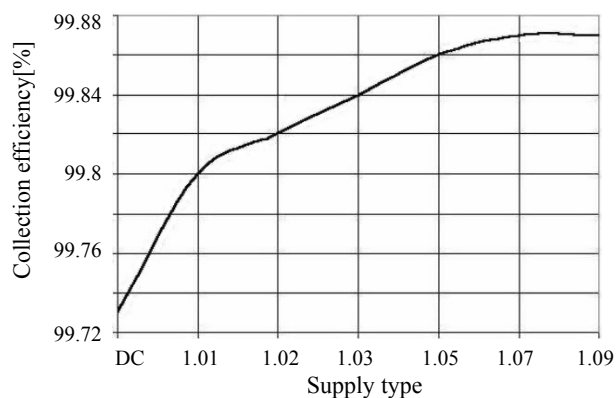


Fig.9. Collection efficiency depending on types of sections energizations

The growing up of discharge wires number from electrostatic precipitator sections ducts has a positive effect on electrostatic precipitator performances, however involves a supplementary price. A bigger value of distance between the discharge wires and collecting plate causes increase of collecting efficiency, but involves more performance electrical isolations and power supplies with bigger voltages. Increasing of intermitence of electrostatic precipitator sections power supplies causes increasing of collection efficiency (especially for high resistivity fly ash).

5 Mathematical models for current-voltage characteristics

The current-voltage characteristics are very important to estimate the collection efficiency, the control and the sections power of the ESPs. The analytic current-voltage characteristics made with electric field strength E, particle charge density ρ_s , current density j, ion mobility k_i , with differential equations [4,6,7]:

$$\nabla \bar{E} = \frac{\rho_s}{\epsilon_0}, \tag{16}$$

$$\nabla \bar{j} = 0, \tag{17}$$

$$\bar{E} = -\nabla V, \tag{18}$$

$$\bar{j} = \rho_s \cdot k_i \cdot \bar{E}. \tag{19}$$

The mathematical models have, in general, the following equation for current-voltage characteristics [13]:

$$I = k_i \cdot G \cdot U \cdot (U - U_0), \tag{20}$$

I[A/m] is the specific current, U [V] is the voltage between the electrodes, U_0 [V] is the initial Corona voltage and $G[s/(m^3 \cdot \Omega)]$ is a coefficient that depends by used method.

Method 1 (Deutsch - the distance d[m] between the discharge wires will be neglect)

$$G = \frac{8 \cdot \pi \cdot \epsilon_0}{\left(\frac{4 \cdot s}{\pi}\right)^2 \cdot \ln\left(\frac{4 \cdot s}{\pi \cdot r_e}\right)}, \tag{21}$$

s[m] is the distance between the discharge wire and the collecting plate, r_e [m] is the equivalent radius for the discharge wire.

Method 2 (Deutsch - the distance d[m] between the discharge wires is not be neglect)

$$G = 2 \cdot \pi^3 \cdot \frac{\epsilon_0}{d^2} \cdot A \cdot \left(1 + B \cdot \sqrt{\frac{r_0}{d}}\right). \tag{22}$$

If $0.8 \leq s/d \leq 2.3$ then $A = \frac{0.017}{\frac{s}{d} - 0.585} - 0.007$; $B = 1.75$,

and if $0.5 \leq s/d < 0.8$ then $A = 0.515 - 0.56 \cdot \frac{d}{s}$; $B = 3.5$.

Method 3 (Cooperman)

$$G = \frac{4 \cdot \pi \cdot \epsilon_0 \cdot \frac{1}{s^2}}{\ln \frac{Z}{r_e}} \quad (23)$$

$$Z = \frac{d}{2 \cdot \pi} \cdot e^{\frac{\pi \cdot s}{d}} \quad (24)$$

In a ESP, each section supplies separate:

$$I_{tot} = I_{tot} \cdot k_i \cdot G \cdot U \cdot (U - U_0) \quad (25)$$

I_{tot} is total current through ESP section, l_{tot} is the total length of the discharge wire from a ESP section. The initial Corona voltage for a section of ESP may be compute with [1,6]:

$$U_0 = E_0 \cdot r_e \cdot \ln \frac{m}{r_e} \quad (26)$$

E_0 is a initial electric field strength (27). If $s/d < 0.3$ then $m = \frac{4}{\pi} \cdot s$, if $0.3 \leq s/d < 1$ then

$$m = 0.18 \cdot d \cdot e^{2.96 \frac{s}{d}}, \text{ if } 1 \leq s/d \text{ then } m = \frac{d}{2 \cdot \pi} \cdot e^{\frac{\pi \cdot s}{d}}.$$

Peek proposed a semiempirical relation to find the initial electric field strength E_0 [1,13]:

$$E_0 = A \cdot \delta + B \cdot \sqrt{\frac{\delta}{r_e}} \quad (27)$$

$$\delta = \frac{p_2}{p_1} \cdot \frac{T_1}{T_2} \quad (28)$$

$\delta[-]$ is the relative density of gas, $A[V/m]$ is a constant that depends of gas and $B[V/m^{0.5}]$ is a constant that depends the Corona polarity, $p_1=10^5 [N/m^2]$ is the pressure at temperature $T_1=273 [K]$, and $p_2 [N/m^2]$ is the pressure at temperature T_2 . For the ESP, when it is negative Corona, the constants have the value: $A=3.2 \cdot 10^6 [V/m]$ and $B=9 \cdot 10^4 [V/m^{0.5}]$.

6 Comparative analyze of the measurement and compute characteristics

For an ESP with four section from a thermal power plant where made graphics currents depending on voltages measured [22] and computed with three methods (methods 1,2,3) using equations (21)-(25). Each of the ESP section has the following characteristics: $s=0.175[m]$, $d=0.14[m]$ ($s/d=1.25$), $r_e=0.75[mm]$, $l_{tot}=8280[m]$.

At power plant, a generating set (with maximum 200MW) has two ESPs (noted with A and B). Were measured the currents and the voltages, for each sections of an ESP, for a minimum load (electrical power of generating set 145-150 MW, $t_{gas}=142.5 ^\circ C$) and for a maximum load (electrical power of generating set 175-190 MW, $t_{gas} = 150 ^\circ C$) [2,24,25].

The measured and computed current-voltage characteristics are present in fig.10-17 for a minimum and maximum load, for every section.

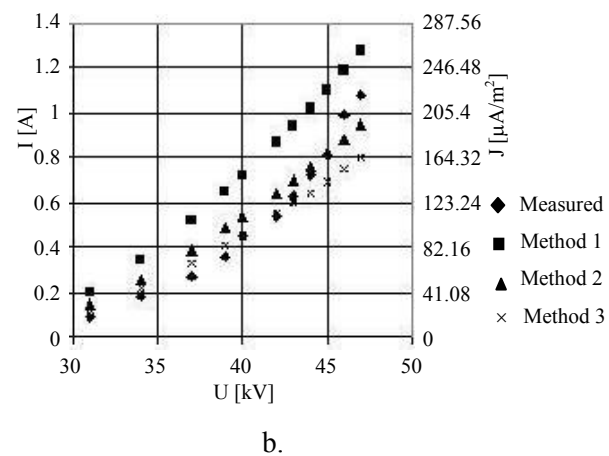
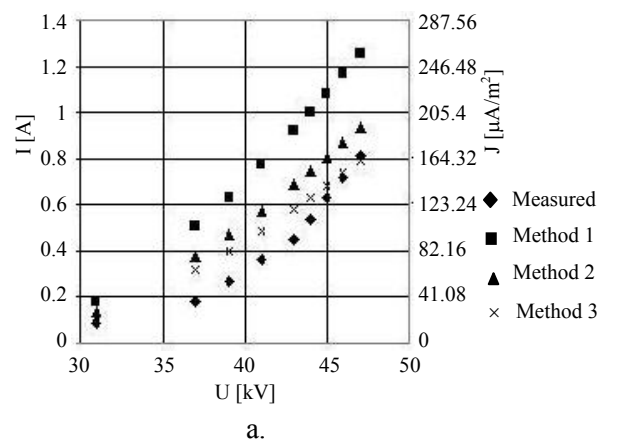
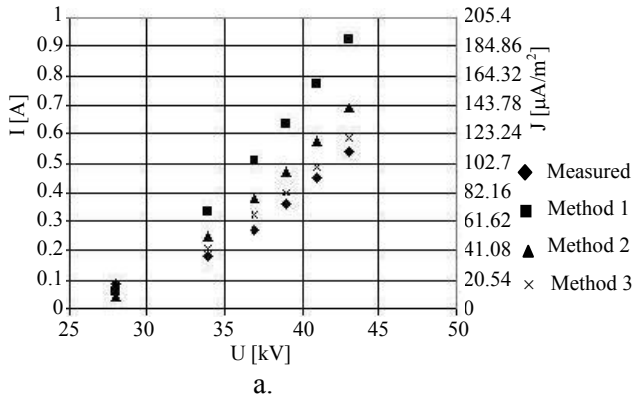
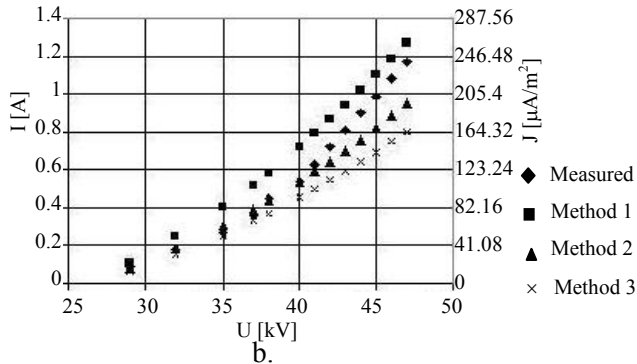


Fig. 10. Current-voltage characteristics for ESP 1A at minimum (a) and maximum (b) load: section 1

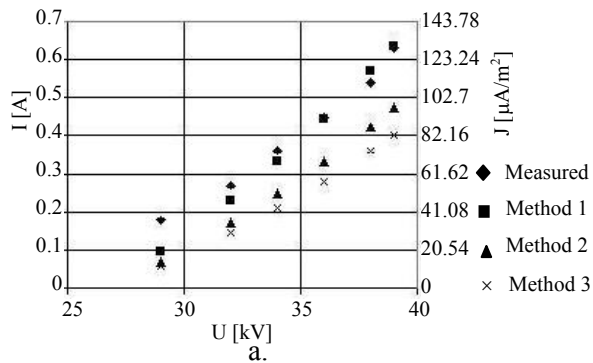


a.

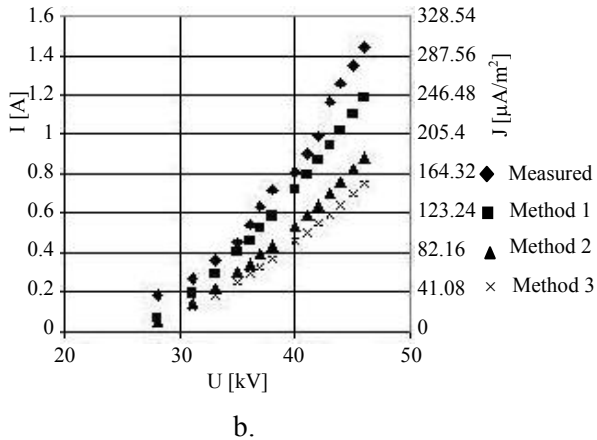


b.

Fig. 11. Current-voltage characteristics for ESP 1A at minimum (a) and maximum (b) load: section 2

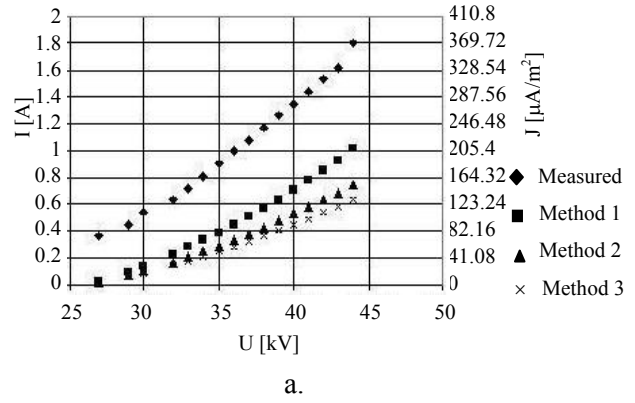


a.

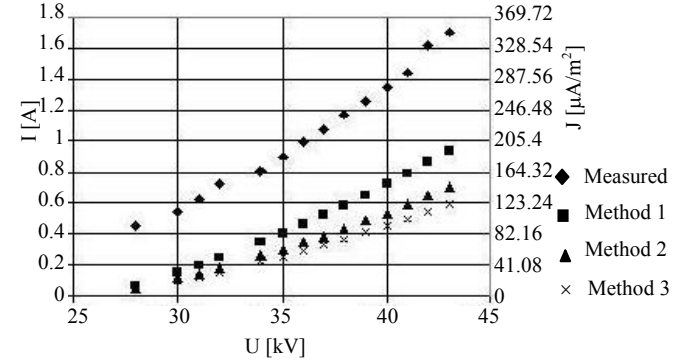


b.

Fig. 12. Current-voltage characteristics for ESP 1A at minimum (a) and maximum (b) load: section 3

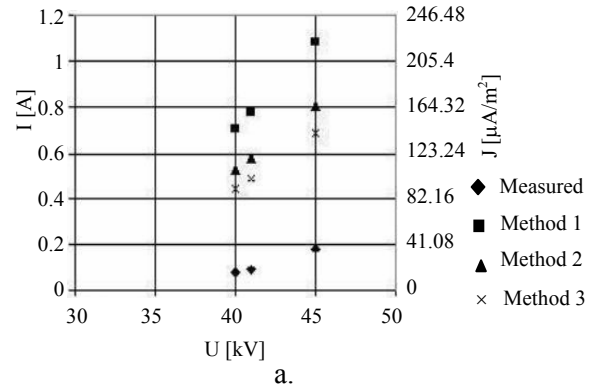


a.

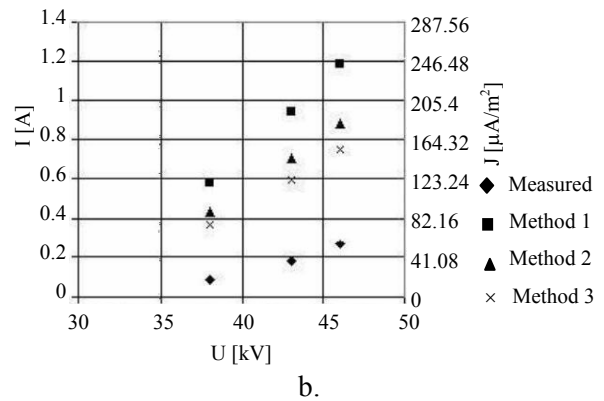


b.

Fig. 13. Current-voltage characteristics for ESP 1A at minimum (a) and maximum (b) load: section 4

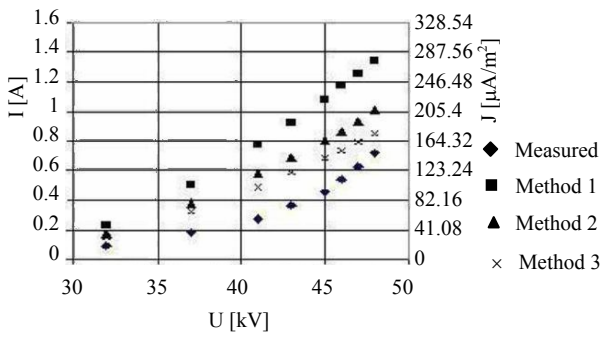


a.

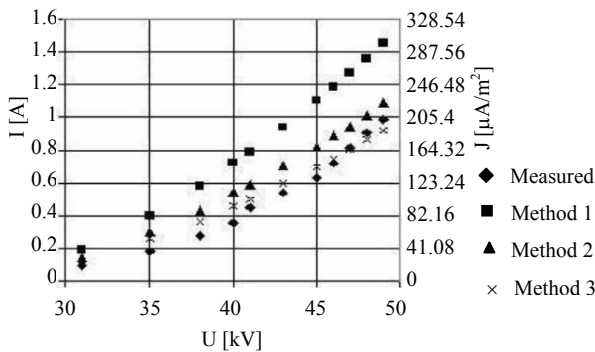


b.

Fig. 14. Current-voltage characteristics for ESP 1B at minimum (a) and maximum (b) load: section 1

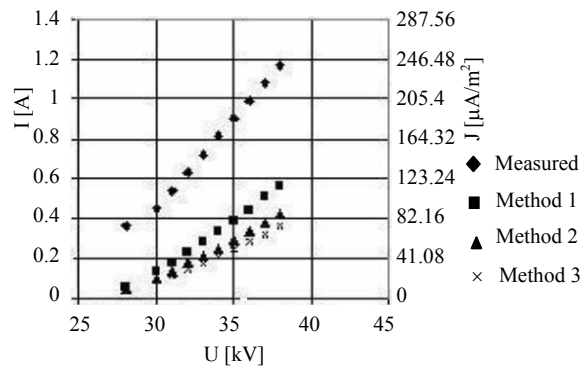


a.

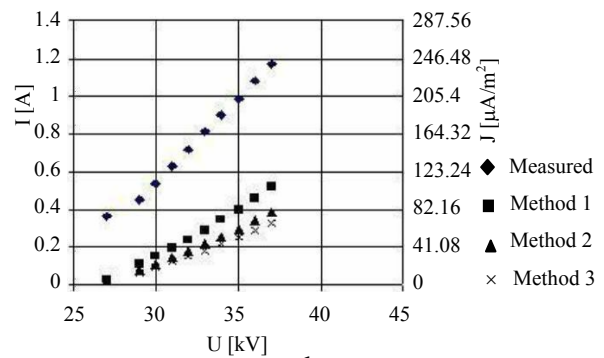


b.

Fig. 15. Current-voltage characteristics for ESP 1B at minimum (a) and maximum (b) load: section 2

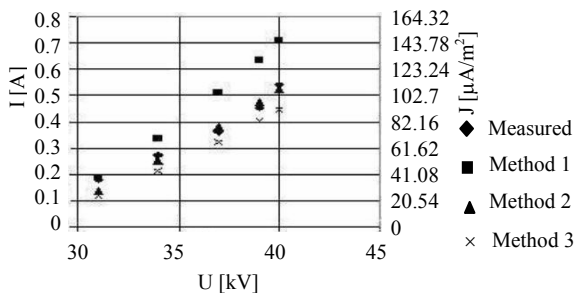


a.

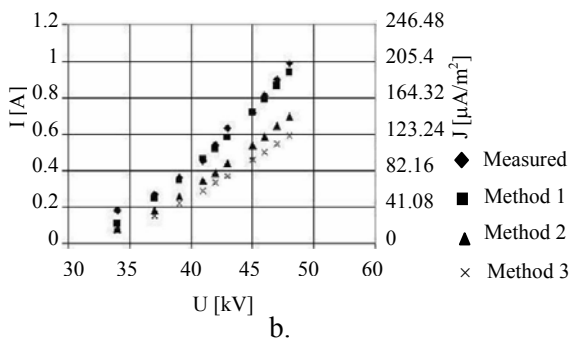


b.

Fig. 17. Current-voltage characteristics for ESP 1B at minimum (a) and maximum (b) load: section 4



a.



b.

Fig. 16. Current-voltage characteristics for ESP 1B at minimum (a) and maximum (b) load: section 3

After the study of current-voltage characteristics from fig.10-17 for minimum and maximum load, the best compute current-voltage characteristics are for sections 2 and 3. It can not be specify that methods (1 or 2 or 3) are better. For minimum and maximum load, for a specify method, the results of compute characteristics are close. The on set Corona voltages have big values at the input sections and have smaller values at the output sections of ESP. At the same time with gas cleaning, the onset Corona voltage in a clean gas (towards output sections) has small values. The discharge voltages in the ESP sections are bigger in the input sections comparative with output sections.

For the same sections, the breakdown voltages, in general increase with dust concentration (at section 1 and 2). The smaller values of breakdown voltages from sections (3 and 4) are present because fault control of voltages from section or unproper alignment of discharge wires.

7 Conclusion

It was determined the maximum distance until the ions are moved, with (7). If alternating field frequency decreases, the maximum distance increases (fig.1). The ESP supply is not efficient only with alternative voltage because it occurs an oscillation trajectory of electric charge dust particles. If it overtakes a limit of voltage frequency, the oscillation amplitude of charge dust particles is lower than the distance between electrodes.

Were analyzed ten cases for industrial ESP operating in a thermal power station, the relative errors of collection efficiency, compared with real measurements, are very small (table 4). These errors show the model performances used by ESPVI 4.0.a software.

The migration velocity and the collection efficiency (fig.6) have small values for particles with diameter under 5 [μm] and have big values for particles with diameter over 10 [μm], when the supplies of ESP sections were made with traditional energization.

To improve the collecting performances of ESP, from the analysis solutions (table 4), a useful method is to use special devices to achieve an intermittent power supplies (intermittent energization) for middle and outlet section where is high resistivity fly ash. With this method the collection efficiency increases and the electric energy consumption decreases. This solution is valid when collecting dust with high resistivity ($> 10^{11}$ [$\Omega\cdot\text{cm}$]).

The growing up of discharge wires number from the sections ducts (fig.7) determines a little increase of collection efficiency, but the cost, mount and maintenance prices increase.

The increasing of distance between the discharge wires and the collecting plates (fig.8), causes a light increasing of collection efficiency, but must upgrade ESP sections, replaced the electrical isolations and power supplies (to obtain a higher voltage).

Through different types of ESP power supplies sections can considerably improve the collection efficiency of ESPs. Depending on the dust and gas properties for each ESP section, by choosing the right combination of power supplies and process control the ESP efficiency can be improved.

For an ESP from industry (a thermal power plant) for a minimum and a maximum load (for two power of no.1 generating set) was made comparison between measured and computed (with (20)-(25)) current-voltage characteristics. The best modelling of current-voltage characteristics are for sections 2,3 (middle section) for ESP 1A and ESP 1B. For sections 1,4 (inlet and outlet section) the

mathematical modeling of characteristics is unsatisfactory because the ESP works in industrial conditions (unproper alignment of discharge wires, the absence of some discharge wires from sections, some semisections are not supplied, fault control of Corona power at discharge wires) and some parameters used in models were approximate (E_0 , U_0 , k_i , r_e).

It is important to predict the current-voltage characteristics for ESP sections because can be used to control corona power, to optimize the spark rate, to optimize the rapping sequences and to control the energy management system. To compute realistic current-voltage characteristics is necessary to estimate the corona current injected in ionization region as a function of applied amplitude and shape voltage and depending on configuration of discharge wires. Also, it is necessary to use a comprehensive negative corona model that involved various phenomena like: glow corona, Trichel pulses, sparking, breakdown streamers, etc.

References:

- [1] K.R. Parker, *Applied Electrostatic Precipitation*, Chapman and Hall, London, U.K., 1997.
- [2] G.N. Popa, *Contributions to Improving Performances of Plate-Type Electrostatic Precipitators for Bi-Phase Systems Gases-Solid Particles*, PhD Thesis, "Politehnica" University Timișoara, Romania, 2004, (in Romanian).
- [3] E. Rothery, *Atmospheric Emissions Control Techniques for Industrial Applications, the 1st International Conference on Environmental Management and Technologies*, Cairo, Egypt, 1997, pp.1-11.
- [4] E. Lami, F. Mattachini, R. Sala, H. Vigl, A Mathematical Model of Electrostatic Field in Wires-Plate Electrostatic Precipitators, *Journal of Electrostatics*, no.39, 1997, pp.1-21.
- [5] E. Kuffel, W.S. Zaengl, J. Kuffel, *High Voltage Engineering. Fundamentals*, Linacre House, Jordan Hill, Oxford, U.K., 2000.
- [6] A. Medlin, *Electrohydrodynamic Modelling of Fine Particle Collection in Electrostatic Precipitators*, PhD Thesis, School of Physics, University of New South Wales, Australia, 1998.
- [7] E. Lami, F. Mattachini, I. Gallimberti, R. Turri, U. Tromboni, A Numerical Procedure for Computing the Voltage-Current Characteristics in Electrostatic Precipitator Configurations, *Journal of Electrostatics*, vol.34, pp.385-399, 1995.
- [8] M.R. Talaie, M. Taheri, J. Fathikaljahi, A New Method to Evaluate the Voltage-Current

- Characteristics Applicable for a Single-Stage Electrostatic Precipitator, *Journal of Electrostatics*, no.53, 2001, pp.221-233.
- [9] H.J. Schmid, E. Schmid, Investigations in to the Local Mass Flux of Dust to be Precipitated at the Collecting Electrode, *the 6th International Conference on Electrostatic Precipitators*, Budapest, Hungary, 1996.
- [10] N. Grass, Application of Different Types of High-Voltage Supplies on Industrial Electrostatic Precipitators, *IEEE Transactions on Industry Applications*, vol.40, no.6, november/december, 2004, pp.1513-1520.
- [11] N.Y.A. Shammas, S. Eio, D. Chamund, Semiconductor Devices and Their Use in Power Electronic Applications, *WSEAS Transactions on Power Systems*, Issue 4, Volume 3, April 2008, pp. 128-140.
- [12] M. Jędrusik, J.B. Gajewski, A.J. Świerczok, Effect of the Particle Diameter and Corona Electrode Geometry on the Particle Migration Velocity in Electrostatic Precipitators, *Journal of Electrostatics*, no.51-52, 2001, pp.245-251.
- [13] S.M. Digă, *Contribution on Electrostatic Precipitators Improving Performances*, PhD Thesis, Politechnica University București, Romania, 1998, (in Romanian).
- [14] R.T. Truce, W. Reibelt, New Technology Improves Electrostatic Precipitator Performance, *the 7th International Conference on Electrostatic Precipitators*, Kyongju, South Korea, 1998.
- [15] M. Jedrusik, J. Jedrusik, Exploitation Experience of the Cooperation of an Electrostatic Precipitator and a Desulphurisation Installation, *the 6th International Conference on Electrostatic Precipitators*, Budapest, Hungary, 1996.
- [16] Z. Yanlei, Research and Implementation of a Novel DC High Voltage Power Supply, *WSEAS Transactions on Circuits and Systems*, Issue 2, Volume 7, February 2008, pp. 55-60.
- [17] H. Tatizawa, G.F. Burani, P.F. Obase, Application of Computer Simulation for the Design of a New High Voltage Transducer, Aiming to High Voltage Measurements at Field, for DC Measurements and Power Quality Studies, *WSEAS Transactions on Systems*, Issue 5, Volume 7, May 2008, pp.580-589.
- [18] N. Plaks, Improving Collection of Toxic Fine Particles in ESPs, *the 6th International Conference on Electrostatic Precipitators*, Budapest, Hungary, 1996.
- [19] N. Grass, Fuzzy Logic-Based Power Control System for Multi Field Electrostatic Precipitators, *IEEE Transactions on Industry Applications*, vol.38, no.5, september/october, 2002, pp.1190-1195.
- [20] B. Navarrete, L. Cañadas, V. Cortés, L. Salvador, J. Galindo, Influence of Plate Spacing and Ash resistivity on the Efficiency of Electrostatic Precipitators, *Journal of Electrostatics*, no.39, 1997, pp.65-81.
- [21] ***, *ESPVI 4.0.a. Performance Prediction Model*, National Technical Information Service, U.S.A., 1996.
- [22] ***, *Operation Optimization of ESP no.1 with 4 sections*, Thermal Power Plant Mintia Deva, contract no.7815-1/1998, S.C. ICPET S.A., Bucharest, Romania, 1998.
- [23] V. Vaida, I. Șora, G.N. Popa, The Improving of Plate-Type Electrostatic Precipitators Performances, *National Conference on Power Energy*, Neptun, Romania, 2004.
- [24] ***, *Operation Optimization of ESP no.1 with 4 sections*, Thermal Power Plant Mintia Deva, contract no.7815-1/1998, S.C. ICPET S.A., Bucharest, Romania, 1998.
- [25] I. Șora, G.N. Popa, I. Popa, The Study of Current-Voltage Characteristics for Plate-Type Electrostatic Precipitators, *the 7th International Conference on Applied and Theoretical Electricity*, Băile Herculane, Romania, 2004.